Hum. Reprod. Advance Access published February 20, 2013
Human Reproduction, Vol.0, No.0 pp. 1–13, 2013
doi:10.1093/humrep/det032

human reproduction

ORIGINAL ARTICLE *Infertility*

Morphological and functional preservation of pre-antral follicles after vitrification of macaque ovarian tissue in a closed system

A. Y. Ting[1], R. R. Yeoman[1], J. R. Campos[1,2], M. S. Lawson[1], S. F. Mullen[3], G. M. Fahy[4], and M. B. Zelinski[1,*]

[1]Division of Reproductive and Developmental Sciences, Oregon National Primate Research Center, Beaverton, OR 97006, USA [2]Department of Obstetrics and Gynecology, Faculty of Medicine of Ribeirão Preto, University of São Paulo, Ribeirão Preto, SP, Brazil [3]The World Egg Bank, Phoenix, AZ 85018, USA [4]21st Century Medicine, Inc., 14960 Hilton Dr, Fontana CA 92336, USA

*Correspondence address. Tel: +1-503-690-5367; Fax: +1-503-690-5563; E-mail: zelinski@ohsu.edu

Submitted on November 15, 2012; resubmitted on January 7, 2013; accepted on January 24, 2013

STUDY QUESTION: What are the appropriate conditions to vitrify the macaque ovarian cortex in a large-volume, closed system that will preserve functional pre-antral follicles?

SUMMARY ANSWER: The combination of glycerol, ethylene glycol (EG) and polymers with cooling in liquid nitrogen (LN_2) vapor and a two-step warming procedure was able to preserve tissue and follicle morphology as well as function of a small population of secondary follicles in the macaque ovarian cortex following vitrification in a closed system.

WHAT IS KNOWN ALREADY: For prepubertal cancer patients or those who require immediate cancer therapy, ovarian tissue cryopreservation offers the only hope for future fertility. However, the efficacy of live birth from the transplantation of cryopreserved ovarian tissue is still unclear. In addition, live birth from cryopreserved ovarian tissue has only been demonstrated after tissue autotransplantation, which poses the risk of transmitting metastatic cancer cells back to the cancer survivor in certain cancers.

STUDY DESIGN, SIZE, DURATION: Non-human primate model, $n = 4$, randomized, control versus treatment. End-points were collected from tissue histology, tissue culture (48 h) and isolated secondary follicle culture (6 weeks).

PARTICIPANTS/MATERIALS, SETTING, METHODS: Two vitrification solutions (VSs) containing EG + glycerol (VEG) and EG + dimethylsulfoxide (VED) were examined for vitrification, devitrification and thermodynamic properties. Once the optimal VS was determined, macaque ovarian cortical pieces ($3 \times 3 \times 0.5$ mm^3) were divided into fresh and two vitrified groups (VEG and VED). For the vitrification groups, tissues were exposed to 1/4, 1/2 and 1× VS for 5 min/step as well as 1× VS + polymers for 1 min at 37°C, loaded into high-security straws with 1 ml of VS + polymers, heat sealed and cooled in LN_2 vapor. Samples were warmed in a 40°C water bath and cryoprotective agents were diluted with 1, 0.5, 0.25 and 0 M sucrose. Tissues were fixed for histological analysis and cultured with bromodeoxyuridine (BrdU). Secondary follicles from VEG tissues were encapsulated and cultured ($n = 24$/treatment/animal). Follicle health, diameter and steroid [progesterone, androstenedione (A_4), estradiol (E_2)] production were analyzed weekly.

MAIN RESULTS AND THE ROLE OF CHANCE: Dense stroma and intact pre-antral follicles were observed using VS containing 27% glycerol, 27% EG and 0.8% polymers with cooling in LN_2 vapor and a two-step warming. Higher cooling and warming rates led to fracturing. BrdU uptake was evident in granulosa cells of growing follicles in fresh and vitrified tissues. Secondary follicles from fresh tissues (70 ± 12%) and tissues vitrified with VEG (52 ± 2%) showed similar survival rates (all data: mean ± SEM; $P > 0.05$). For both groups, the initial follicle diameter was similar and increased ($P < 0.05$) by Week 3, but diameters in vitrified follicles were smaller ($P < 0.05$) by Week 6 (566 ± 27 μm) than those of the fresh follicles (757 ± 26 μm). Antrum formation rates were lower ($P < 0.05$) for vitrified (37 ± 6%) relative to fresh (64 ± 8%) follicles. There was no significant change in levels in culture media of E_2, P_4 and A_4 between fresh and VEG groups at any time point during culture.

LIMITATIONS, REASONS FOR CAUTION: Only *in vitro* studies are reported. Future *in vivo* tissue transplantation studies will be needed to confirm long-term function and fertility potential of vitrified ovarian tissues.

WIDER IMPLICATIONS OF THE FINDINGS: This is the first demonstration of antral follicle development during 3D culture following ovarian tissue vitrification in a closed system using primate ovarian tissue. While diminished antrum formation and slower growth *in vitro* reflect residual cryodamage, continued development of ovarian tissue vitrification based on cryobiology principles using a non-human primate model will identify safe, practical and efficient protocols for eventual clinical use. Tissue function following heterotopic transplantation is currently being examined.

STUDY FUNDING/COMPETING INTEREST(S): National Institutes of Health (NIH) Oncofertility Consortium UL1 RR024926 (1RL1-HD058293, HD058295, PL1 EB008542), the Eunice Kennedy Shriver NICHD/NIH (U54 HD018185) and ONPRC 8P51OD011092-53. G.M.F. works for the company that makes the polymers used in the current study.

Key words: ovary / vitrification / primate / follicle culture / cryopreservation

Introduction

The 5-year survival rate for women under 45-year old diagnosed with cancer is 83% (Howlader *et al.*, 2012). With advanced detection tools, patients are now diagnosed and treated for cancer at a younger age and are more likely to survive. However, cancer treatments, such as chemotherapy, radiation and/or bone marrow transplantation, can deplete follicles in the ovary leading to premature ovarian failure, infertility and long-term health risks associated with menopause (Schmidt *et al.*, 2010). Cryopreservation of embryos, oocytes and ovarian tissue (Jeruss and Woodruff, 2009) is available to preserve fertility in female patients with cancer. Although embryo freezing is currently the only established method, ovarian tissue cryopreservation has emerged as a promising hope for future fertility for patients who are pre-pubertal or require immediate cancer therapy. Autografting of cryopreserved ovarian tissue also restored ovarian endocrine function in almost every case reported (Rosendahl *et al.*, 2011; Silber, 2012), including induction of puberty (Poirot *et al.*, 2012).

Unlike the robust return of endocrine functions, there are only 22 documented live births following the transplantation of cryopreserved ovarian tissue since the first reported case in 2004 (Demeestere *et al.*, 2010; for review, see Donnez *et al.*, 2012; Muller *et al.*, 2012). The efficacy of live birth from the transplantation of cryopreserved ovarian tissue is difficult to predict, since lack of pregnancy is rarely reported. Live births were achieved in 2 of 12 women during 10 years and 386 cases of ovarian tissue cryopreservation in Denmark (Rosendahl *et al.*, 2011), demonstrating the lengthy interval involved in collecting sufficient data. All reported live births have resulted from ovarian tissue cryopreserved using a slow freeze protocol. This method utilizes low concentrations of cryoprotective agents (CPAs) and a gradual decrease in temperature to favor extracellular and avoid intracellular, ice formation (Mazur, 2004). Vitrification utilizes relatively high CPA concentrations and with proper cooling and warming rates, it results in a glassy state without intracellular or extracellular ice (Fahy *et al.*, 1984). Recent advances in embryo and oocyte cryopreservation suggest that vitrification yields better results in comparison with slow freezing (Abdelhafez *et al.*, 2010; Cobo and Diaz, 2011; Martinez-Burgos *et al.*, 2011). In addition, vitrification is sometimes favored over slow freezing, because it can be less time-consuming, more economical and performed in virtually any laboratory. However, a standard protocol for ovarian tissue vitrification that demonstrates consistent outcomes is lacking (Amorim *et al.*, 2011), and no data from the transplantation of vitrified ovarian tissue in women have been reported.

The limited progress for ovarian tissue vitrification is largely due to the complex physical and biological properties of the ovary as well as some practical challenges. Ovarian tissue contains a variety of cell types that vary in size, membrane permeability, distribution and abundance. Ovarian tissue cannot be visually monitored at a cellular level during the vitrification process for the osmotic change and cellular influx of CPAs. Other challenges include the limited amount of human ovarian tissue for research and lack of an immediate functional end-point. Pooled samples from different patients of various ages and reproductive backgrounds are often used in a single study, resulting in a lack of systematic comparison. Currently, the most common methods for evaluation of cryopreserved ovarian tissue are morphology and immunohistochemical localization of protein markers for proliferation and apoptosis; however, these end-points do not reflect true ovarian function. The gold standard for the success of a fertility preservation method is live birth, which can take several years to achieve.

Because most protocols for ovarian tissue vitrification are adapted from those of embryos and oocytes (Amorim *et al.*, 2011) and use empirical approaches due to limited samples; thus far, little effort has been made using basic vitrification principles. For oocytes and embryos, the minimal sample volume and the maximum cooling rate are often used to achieve vitrification with relatively low CPA concentrations (Yavin and Arav, 2007). A similar approach has been followed in ovarian tissue vitrification by directly plunging the tissue into liquid nitrogen (LN_2). However, this open system poses a safety risk for possible contamination from direct contact of tissue with LN_2 as well as cross contamination between specimens during storage (Bielanski and Vajta, 2009). Since the critical CPA concentration to achieve a vitreous state is positively correlated with the sample volume and negatively correlated with the cooling rate, it is important to determine the minimum CPA concentration needed for a given sample volume to achieve vitrification, but also to avoid devitrification that occurs when a formerly vitrified solution forms ice during warming. Cooling and warming rates should also be optimized for practicality and to avoid fracturing in a larger volume sample (Fahy *et al.*, 1984; de Graaf *et al.*, 2007).

Since a relatively high concentration of CPAs is required for vitrification, a combination of two or more permeating CPAs is commonly used to minimize toxicity. Both ethylene glycol (EG) and dimethylsulfoxide (DMSO) have been used frequently in embryo, oocyte and ovarian tissue cryopreservation (Kagawa *et al.*, 2009). The use of glycerol and EG showed low toxicity in embryos (Ali and Shelton, 1993) and has been used for ovarian tissue vitrification with promising results

(Isachenko *et al.*, 2002; Ting *et al.*, 2012). In addition to permeating CPAs, the addition of one (Hashimoto *et al.*, 2010; Amorim *et al.*, 2012) or a combination (Ting *et al.*, 2012) of non-permeating polymers, such as polyvinylpyrrolidone (PVP), a specific copolymer of polyvinylalcohol and polyvinylacetate (PVA; Supercool X-1000^{TM}) and polyglycerol (Supercool Z-1000^{TM}) (Wowk *et al.*, 2000), improved the outcome for vitrified macaque ovarian tissue.

Using a non-human primate model, the current study carefully describes a closed system for the vitrification of ovarian tissue using a hermetically sealed high-security straw. Two combinations of permeating CPAs (EG + glycerol and EG + DMSO) were examined for their ability to vitrify without apparent devitrification at different concentrations and different cooling and warming rates. Fresh and vitrified tissues were examined histologically as well as for cellular proliferation via bromodeoxyuridine (BrdU) uptake. Secondary follicles were isolated from fresh and vitrified (optimal protocol) ovarian tissue for encapsulated 3D culture as an indicator of follicular function.

Materials and Methods

Animals and ovary collection

'The general care and housing of rhesus macaques (*Macaca mulatta*) at the Oregon National Primate Research Center (ONPRC) has been previously described (Wolf *et al.*, 1990). Briefly, animals were caged in pairs in a temperature-controlled (22°C) light-regulated 12L:12D room and fed food and water *ad libitum*. The studies were conducted in accordance with the National Institutes of Health Guide for the Care and Use of Laboratory Animals and all protocols were approved by the ONPRC Animal Care and Use Committee. Ovaries were collected by laparoscopy from anesthetized adult female rhesus monkeys ($n = 8$) exhibiting normal reproductive cycles' (Ting *et al.*, 2012). A blood sample during the early follicular phase on Days 2–5 of the menstrual cycle (Day 1 = first day of menses) was collected prior to ovariectomy for estradiol (E_2) and progesterone measurements. Four animals (10.5-year old; $E_2 = 35 \pm 8$ pg/ml; progesterone = 0.15 ± 0.06 ng/ml) were used to examine tissue histology using different vitrification solutions (VSs) and for tissue culture. Once the better VS was determined, four additional animals (6–10-year old; $E_2 = 46 \pm 10$ pg/ml; progesterone = 0.17 ± 0.09 ng/ml) were used for follicle quantification and 3D follicle culture. 'Ovaries were placed into 3-(*N*-morpholino) propanesulfonic acid (MOPS)-buffered tissue holding media (HM; CooperSurgical Inc., Trumbull, CT, USA) and immediately transported to the laboratory at 37°C. All chemicals were purchased from Sigma (St Louis, MO, USA) unless otherwise stated.' (Ting *et al.*, 2012)

Ovarian tissue processing

Ovaries were processed in HM supplemented with 15% (v/v) serum protein substitute (SPS, CooperSurgical Inc.) and 29 μg/ml of the antioxidant L-ascorbic acid 2-phosphate sesquimagnesium salt hydrate (ascorbic acid phosphate) as described previously (Ting *et al.*, 2012). Following the removal of fatty and non-ovarian tissue by trimming, 0.5 mm thick outermost ovarian cortical pieces were collected using a Stadie-Riggs tissue slicer (Thomas Scientific, Swedesboro, NJ, USA). Ovarian cortex slices were cut into 3×3 mm^2 fragments using a scalpel. Owing to the heterogeneous follicle distribution in the primate ovary, only tissues ($n = 28 \pm 2$ pieces/animal) with the presence of secondary follicles, as determined under a dissecting scope, were selected for further analysis. For each animal, tissues were randomly divided into fresh and vitrification groups (8–12 pieces/group). We utilized a randomized block design for the current set of experiments; hence, each animal contributed equally to each treatment group and all evaluation end-points. Ovarian tissue was handled and processed at 37°C.

Determining VS concentration

Two formulations for the VS were used in the current study: 'VEG' EG + glycerol and 'VED' EG + DMSO. Equal parts of CPAs were used in both protocols and all solutions were measured by weight. The tested concentrations of VS included 40, 45, 50, 51, 52, 53, 54 and 55% (w/v) total CPA. For example, 50% VEG contains 25% EG and 25% glycerol. All solutions were made in HM supplemented with non-permeating CPA polymers (0.2% [w/v] PVP K-12, 0.2% SuperCool X-1000^{TM} and 0.4% SuperCool Z-1000^{TM}; 21st Century Medicine, Fontana, CA, USA) (Wowk *et al.*, 2000; Ting *et al.*, 2012), 15% (w/v) SPS and 29 μg/ml ascorbic acid phosphate. To determine the minimal concentration needed for the solution to vitrify in a closed system without apparent devitrification or re-crystallization, tissue straws (CryoBio System; 2 ml high-security tissue straw; cut into half; Fig. 1a) were heat sealed at one end, 1 ml of VS was loaded into each straw and the open end was heat sealed (Fig. 1b). Two practical cooling rates were carried out by direct plunging of VS-filled straws into LN_2 (fast cooling) or cooled in LN_2 vapor (slow cooling). Two warming rates were achieved by submerging of vitrified samples directly into a 40°C water bath (fast warming) or exposing the sample first to room temperature air (in the current study, room temperature is 30°C in the warm room) and then submerging into a 40°C water bath (slow warming). The LN_2 vapor environment was created by placing a tube rack flat inside a Styrofoam box and filling the box with LN_2 1–5 cm below the top of the rack (temperature at the top of the rack = 180 ± 3°C). Sealed straws were then placed on the top of the rack to cool. The ability for each VS to vitrify during cooling as well as the presence or the absence of devitrification or re-crystallization during warming was recorded.

Cooling and warming rates and thermodynamic properties of VEG and VED

VS temperature was measured using a digital thermocouple thermometer (SATO, SK-1100, Tokyo, Japan) during cooling and warming every 10 and 5 s, respectively. The measurement was repeated three times, linear regression was calculated and cooling as well as warming rates were determined. Cooling and warming thermograms were obtained with a differential scanning calorimeter (DSC 7; Perkin Elmer, Waltham, MA, USA) running with Pyris software (version 3.81, Fahy *et al.*, 2004) as described previously (Wowk *et al.*, 2000). Briefly, 'liquid samples of ~15 mg mass were crimped in aluminum sample pans (Perkin Elmer) and placed in the DSC sample oven for analysis. An empty sample pan was kept in the DSC reference oven to balance the instrument. DSC was calibrated by measuring the onset of the crystal transition of cyclohexane at −87.06°C while warming at 2°C/min and the onset of melting curve of a known mass of water ice (334 J/g nominal)' (Wowk *et al.*, 2000). Analyses were conducted at a cooling rate of 35°C/min from 10 to −160°C (machine limit). Steps for warming include (i) heat from −160.00 to −110.00°C at 90.00°C/min and (ii) heat from −110.00 to 10.00°C at 300.00°C/min. Values for the glass transition temperature (T_g) were extrapolated as the midpoint of the change in heat capacity, C_p, associated with the glass transition. Cooling and warming thermal scans were repeated in triplicate for VEG and VED.

Vitrification and warming

Ovarian tissues ($n = 8$-12/group/animal) were incubated sequentially in 1/4 equilibration solution (ES, w/v), 1/2 ES and 1× ES containing 27%

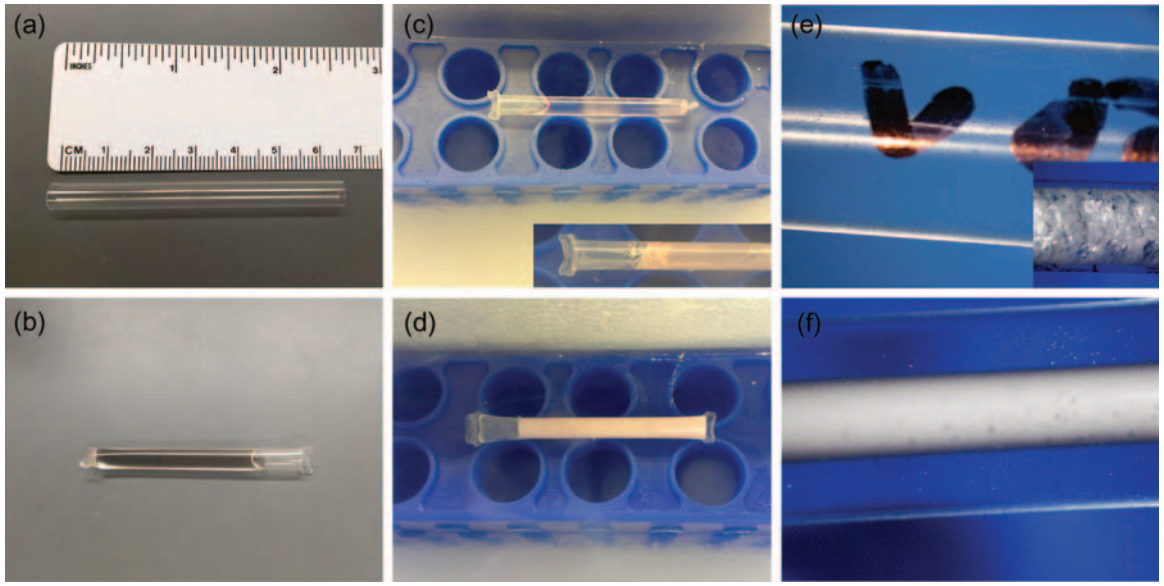

Figure 1 The vitrification straw and examples of the process used for macaque ovarian tissue. A high-security tissue straw (diameter = 6 mm, length = 65 mm) before (**a**) and after (**b**) VS loading and heat seal. During cooling in LN_2 vapor, VS with sufficient concentrations of CPAs vitrified (**c**), whereas VS with inadequate CPA formed ice crystals (**d**). During the two-step warming procedure, immediately after samples are plunged into a warm water bath, VS with sufficient CPAs did not show devitrification (**e**), whereas previously vitrified VS with inadequate CPA formed ice during warming (**f**). Rapid cooling (directly into LN_2) and warming (directly into a water bath) caused extensive fracture (c and e, inserts).

EG (3.2 M) + 27% glycerol (4.7 M; VEG) or 25.5% EG (3 M) + 25.5% DMSO (4.5 M; VED). ES contains permeating CPAs in HM supplemented with 15% SPS and 29 μg/ml of ascorbic acid phosphate, whereas VS contains ES plus polymers. Tissues in the VEG group were exposed first in a solution containing 5% glycerol (0.6 M) prior to 1/4 ES owing to the low permeability of glycerol followed by transfer into VS. Tissues were incubated at 37°C for 5 min in each ES followed by 1 min in the VS. In preliminary studies (data not shown), we examined different equilibration times (3, 5 and 10 min per step). When tissues were equilibrated for 3 min per step, tissue did not vitrify during cooling. When tissues were incubated for 10 min per step, tissue toxicity was observed. Results showed that the 5-min incubation time allows vitrification and minimal toxicity of the ovarian tissue of the same size. Tissues ($n = 3–8$/straw) were then transferred into labeled straws pre-loaded with 1 ml of VS + polymers. Straws were heat sealed, placed in LN_2 vapor for 10 min (the temperature of VS reached approximately −180°C) and transferred into LN_2 for storage. All tissues vitrified in the straw regardless of the number of tissues per straw, and we did not see any difference in tissues from the straws with different numbers of fragments.

For warming, each straw was individually removed from LN_2, exposed to room temperature air (30°C) for 1 min (the temperature of VS reached approximately −100°C), followed by plunging into a 40°C water bath for 30 s (the temperature of VS reached ~25°C). Tissues were released by cutting both ends of the straw and transferred into HM supplemented with 1 M sucrose (1 min), followed by a 5-min incubation in each of 0.75, 0.5 and 0.25 M sucrose solutions, and two 10 min incubations in HM. The incubation time during the CPA removal was based on studies performed by Kagawa *et al.* (2009) and additional dilution steps were added to minimize osmotic stress. Warmed tissues were put into maintenance culture media [alpha Minimum Essential Media (αMEM) supplemented with 3% SPS and 29 μg/ml of ascorbic acid phosphate] at 37°C in 5% CO_2 in atmospheric air for 2 h before fixation. All incubations with vitrification and warming solutions were carried out at 37°C with shaking.

Tissue processing, histology and quantification of pre-antral follicles

Similar to methods published previously (Ting *et al.*, 2012), fresh and vitrified tissues ($n = 4$/group/animal) were fixed in 4% paraformaldehyde at 4°C overnight, processed for paraffin embedding and serial sectioned at 5 μm. Every 20th section was stained with hematoxylin and eosin (H&E) for histological analysis. Secondary follicles were counted and evaluated in each H&E stained section [$n = 4$ animals; 4 pieces/animal; 8–12 sections/piece (100 μm intervals)]. Due to their small size and high numbers per tissue, primordial and primary follicles were counted in three randomly selected microscopic images captured (Olympus BX 40 microscope equipped with DP72 camera and CellSens software, Center Valley, PA, USA) from each H&E stained section using ImageJ (National Institutes of Health, Bethesda, MD, USA). Follicles were evaluated based on oocyte and granulosa cell morphology. Normal follicles were as described previously (Ting *et al.*, 2012) as those exhibiting cell-to-cell contacts between neighboring granulosa cells, and the absence of any contraction of the cytoplasm or pyknotic nuclei in the oocyte or in the granulosa cells. Follicle definition was based on that described by Gougeon (1996). Only follicles with a visible oocyte were included during counting for an accurate estimation of follicular development.

Tissue culture and BrdU uptake

BrdU is incorporated into newly synthesized DNA in dividing cells and was used for the evaluation of post-warm tissue viability in culture (Onions *et al.*, 2008). Fresh and vitrified tissues ($n = 2$/group/animal) were cultured in follicle culture media (defined below) containing BrdU (0 or 50 μM, BD Pharmingen, Franklin Lakes, NJ, USA) for 48 h at 37°C in

5% CO_2 in atmospheric air. Tissues were cultured (one per well) in tissue culture inserts (0.4 μm pore size, EMD Millipore, Billerica, MA, USA) in 24-well culture plates. After 48 h, culture media were collected for hormone measurement. Tissues were fixed, processed and sectioned as described above. Every 30th section was immunostained for BrdU [1:200; mouse monoclonal immunoglobulin (Ig) G, MP Biomedicals, Solon, OH, USA]. Following antigen retrieval, 0.3% H_2O_2, 2 N HCl and serum block treatments, ovarian sections were incubated with non-immune serum or primary antibody against BrdU (1:400; mouse monoclonal IgG, MP Biomedicals) as described previously (Ting *et al.*, 2011). Primary antibody binding was visualized with biotinylated secondary antibodies and 3,3′-diaminobenzidine (Vector, Burlingame, CA, USA). Negative controls included tissue cultured in the absence of BrdU as well as primary antibody omission during the staining protocol.

Secondary follicle culture

A subset ($n = 3–4$ pieces/group/animal) of tissues from fresh and VEG groups were used for secondary follicle isolation and 3D culture. After warming, vitrified tissues were moved into maintenance media at 37°C with 20% O_2. As described previously (Ting *et al.*, 2012), in order to avoid further stress to the vitrified-warmed tissue, tissues were maintained in the culture environment and taken out individually for follicle isolation which can take up to 2 h to complete. In addition, follicle isolation was done mechanically without collagenase treatment. Follicles were isolated from fresh and cryopreserved tissue without collagenase treatment to avoid further damage to follicles. Criteria for the selection of secondary follicles for culture have been described previously (Ting *et al.*, 2012); follicles ($n = 12–24$/group/animal) selected were 120–250 μm in diameter with a round and centrally located oocyte, an intact basement membrane and no antrum formation. 'Individual follicles were encapsulated in 0.25% alginate as previously described (Xu *et al.*, 2010). Briefly, follicles were transferred individually into 5 μl 0.25% (w/v) sterile sodium alginate (in phosphate-buffered saline) and the droplets were crosslinked in 50 mM $CaCl_2$ and 140 mM NaCl solution for 1 min. Encapsulated follicles were rinsed in HM and transferred to individual wells of a 48-well plate containing 300 μl of αMEM supplemented with 2.16 mg/ml glucose, 60 μl/ml SPS, 44 mIU/ml FSH (NV Organon, Oss, Netherlands), 0.5 mg/ml bovine fetuin (fetal plasma protein), 29 μg/ml ascorbic acid phosphate, 5 μg/ml transferrin, 0.5 μg/ml insulin, and 5 ng/ml sodium selenite. Encapsulated follicles were cultured at 37°C in 5% CO_2 in atmospheric air for 6 weeks. Every 2 days, half of the culture media was exchanged with fresh culture media (prepared weekly) and stored at −20°C for subsequent hormonal measurements (Ting *et al.*, 2012)'.

Follicle growth and survival

As described previously, 'during culture, follicle health and diameter were assessed using an Olympus CK40 inverted microscope attached to an Olympus DP11 digital camera. Follicles were considered to be degenerating if (i) the oocyte was no longer surrounded by granulosa cells (the oocyte is separated from and no longer inside the follicular wall), (ii) the oocyte became dark, (iii) the granulosa cells became dark, or (iv) the diameter of the follicle decreased. For each follicle, weekly photographs were taken, and diameters measured using ImageJ. The mean of 2 measurements per follicle (perpendicular to each other) was then calculated and documented as the follicle diameter (Ting *et al.*, 2012)'.

Hormone assays

Concentrations of E_2 and progesterone in serum collected from each animal and E_2, progesterone and A_4 in follicle culture media collected weekly were determined by the Endocrine Technology and Support Core at the ONPRC using an Immulite 2000, a chemiluminescence-based automatic clinical enzyme-linked immunosorbent assay -based platform (Siemens Healthcare Diagnostics, Deerfield, IL, USA). As described previously, 'the sensitivity of assays by the Immulite 2000 is 20 pg/ml for E_2, and 0.2 ng/ml for progesterone. Concentrations of A_4 were measured by radioimmunoassay using a DSL-3800 kit (Diagnostic Systems Laboratories, Inc., Webster, TX, USA) with 0.1 ng/ml sensitivity. The intra-assay and inter-assay coefficients of variation with the Immulite 2000 are <15% for all assays. Data were corrected for culture medium blanks (Ting *et al.*, 2012)'.

Data analysis and statistics

'Data were analyzed by combining observations to make 1 single count per animal giving an equal contribution from each animal and presented as mean ± SEM. For numbers of preantral follicles in H&E sections, data are presented as the average and sum of follicles counted in all 4 animals in each group, and the percentage of follicles in each category relative to the total number of follicles of the same group. Percentages of follicles that exhibit abnormal oocyte or granulosa cells among different treatment groups were analyzed by Chi-square test' (Ting *et al.*, 2012). Tg was extrapolated as the midpoint of the thermal transition during cooling and analyzed using Pyris software.

'For 3D culture, the percentage of follicular survival and antrum formation is presented as percentage rates (mean ± SEM). The 6-week survival and antral formation rate was analyzed using analysis of variance (ANOVA: SigmaPlot 11.0, Systat Software, Inc., San Jose, CA, USA). One-way repeated measures ANOVA was performed for weekly follicle diameter and hormone production within treatments, whereas for data among treatments at a single time point, one way ANOVA was performed. Differences were considered significant when $P \leq 0.05$'(Ting *et al.*, 2012).

Results

Minimal CPA concentration required to vitrify

For VEG, solutions containing 51–55% total permeating CPAs vitrified (turned into glass) during cooling; however, devitrification was absent only with 54 and 55% total permeating CPAs during warming (Fig. 1). For VED, successful vitrification during cooling was observed in 50–55% total permeating CPAs; however, devitrification was absent in solutions with concentration of permeating CPAs of 51% or higher. Therefore, we determined that the minimum concentration needed for 1 ml solution to vitrify without apparent devitrification in the sealed straw is 54% for VEG (27% each of EG and glycerol) and 51% for VED (25.5% each of EG and DMSO).

Cooling and warming rates, Tg and devitrification

The calculated cooling rate for VEG and VED was 37 ± 2 and 36 ± 0.1°C/min, respectively. For the two-phase warming protocol, the calculated warming rate in the air (slow) was 93 ± 2 and 88 ± 2°C/min for VEG and VED, respectively, whereas the calculated warming rate in a water bath (fast) was 372 ± 51 and 419 ± 39°C/min for VEG and VED, respectively. When higher cooling and warming rates were used by plunging the sample directly into LN_2 during cooling and into a warm water bath during warming, extensive fracturing of the solution was observed (Fig. 1c and e inserts).

The observed changes in the heat capacity of VEG and VED during cooling and warming are shown in Fig. 2. On cooling, VEG and VED transitioned to the glassy state (T_g) at -127 ± 0.1 and -134 ± 0.3°C, respectively. The lack of a crystallization peak during cooling on the thermogram indicates that the solution vitrified without ice formation. Warming thermograms showed the glass transition events in VEG and VED occurred between -120 and -110°C (mean T_g values for VEG and VED, -112 ± 0.4 and -115 ± 0.02°C, respectively). These temperatures are higher than those recorded during cooling in part due to the fact that the glass transition is a kinetic rather than a thermodynamic phenomenon and that the warming rate was roughly three times higher than the cooling rate, and some thermal lag exists between the time the glass transition takes place and the time it can be sensed. Immediately after passing through the glass transition, the warming rate was abruptly increased (at -110°C) by more than a factor of 3 to simulate transfer into a warm bath following previous warming in air. This resulted in the expected large sigmoid increase in heat flow into the sample required to change the warming rate and similar to the typical start-up/settling effect seen at the onset of warming at -160°C, but no exothermic peak and subsequent endothermic peak during warming was observed in any case, indicating that devitrification followed by melting was not observed in either VS (Fig. 2).

Histology

Normal morphology of pre-antral follicles was observed in H&E stained sections of fresh ovarian tissue demonstrating contact between the oocyte and surrounding granulosa cells and between

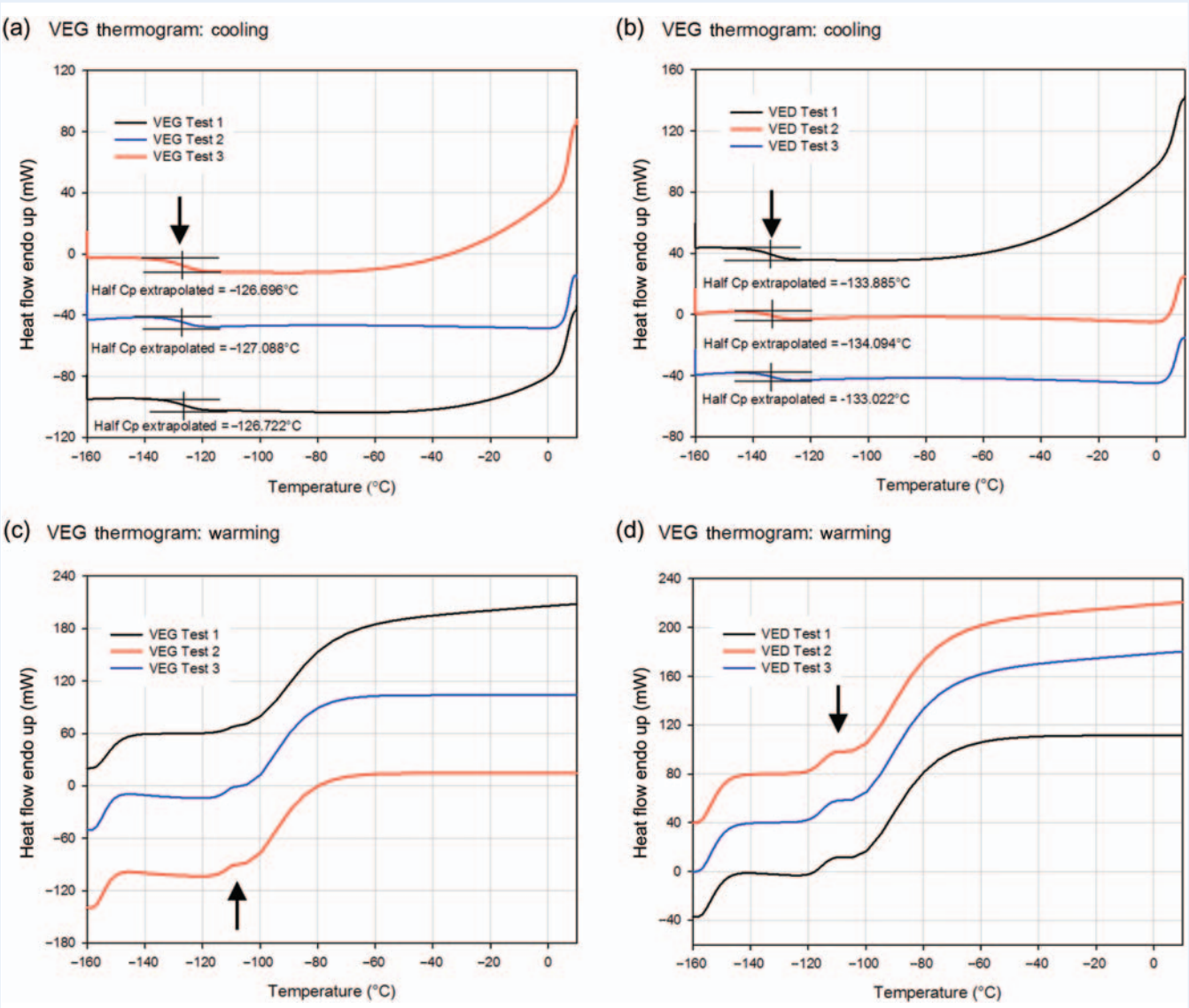

Figure 2 Changes in the heat capacity of VS. Differential scanning calorimeter thermograms during cooling (**a** and **b**) and warming (**c** and **d**) for VEG (a and c) as well as VED (b and d). Glass transition temperature (T_g) was extrapolated as the midpoint of the thermal transition during cooling. The absence of phase transition peaks during cooling and warming validates the lack of crystallization during cooling as well as devitrification and melting during warming for both VSs. Arrows indicate the onset of rapid warming at -110°C, just above the temperature range of the glass transition.

neighboring granulosa cells (Fig. 3a–c). In addition, oocyte cytoplasm in these follicles showed a uniform distribution (Fig. 3b and c). After warming, 3 ± 1% of primordial and primary follicles showed abnormal morphology in the VEG group, similar to that of the fresh (Fig. 4a). On the contrary, 35.4 ± 6.9% of primordial and primary follicles in the VED group showed abnormal morphology, increased in comparison with the fresh (Fig. 4a; $P \leq 0.05$). For secondary follicles, abnormal morphology was found in 30 ± 6, 40 ± 6 and 59 ± 8% oocytes in fresh, VEG and VED groups, respectively (Fig. 4b). Abnormal granulosa cells were found in 8 ± 3, 17 ± 5 and 28 ± 8% secondary follicles of the fresh, VEG and VED groups, respectively (Fig. 4b). Cryo-induced follicular damage included shrunken and vacuolated oocytes, as well as abnormal space between the follicle and stroma. The cortex of fresh tissue (Fig. 3a) and tissues vitrified using both VEG and VED protocols (Fig. 3a, d and g) all had dense and compact stroma.

BrdU culture

BrdU uptake was observed in granulosa cells of primary, secondary and multilayer follicles in fresh tissue (Fig. 5a). BrdU incorporation was also evident in growing follicles in tissues vitrified with VEG (Fig. 5b) and VED (Fig. 5c). Negative controls, including tissue cultured in the absence of BrdU, as well as primary antibody omission during the staining protocol, both showed no positive staining (Fig. 5d). Production of E_2 by cultured tissues was evident in all three groups and seemed reduced following vitrification in both VEG (33 ± 5 ng/ml) and VED (26 ± 13 ng/ml) groups (but was not significant) in comparison with the fresh (78 ± 36 ng/ml).

Encapsulated 3D follicle culture: survival, growth and hormone production

Following histological analysis, only tissue vitrified with VEG was used for secondary follicle culture. Table I summaries survival and antrum formation rates of secondary follicles in 3D culture. The 6-week survival rate of follicles from VEG tissue did not differ ($P > 0.05$) from that of fresh tissue. The proportion of fresh follicles that survived formed an antrum (64 ± 8%) by Weeks 3–4 (Table I; Fig. 6). On the other hand, follicles from VEG tissue showed a reduced (37 ± 6%, $P \leq 0.05$) antrum formation rate in comparison with the fresh, and antrum development was observed by Weeks 3–5 (Table I; Fig. 6).

On the day of isolation, follicle diameters were similar in fresh and VEG groups ($P > 0.05$, 155 ± 5 μm; Figs 6 and 7). Diameters of fresh follicles increased ($P < 0.05$) during Week 2 and continued to grow. Follicle diameters also increased ($P < 0.05$) during Week 2 in follicles from the VEG group. However, the follicle diameters at Week 6 for the VEG group were smaller ($P < 0.05$) when compared with that of the fresh control (Figs 6 and 7). In addition, follicle diameters of the VEG group at Week 6 were similar to that of the fresh follicles at Week 4 (Fig. 7), suggesting a delayed growth.

E_2 production by fresh follicles was elevated ($P < 0.05$) during Week 3 in comparison with Week 0 and continued to rise ($P < 0.05$) to Week 6 (Fig. 7). Levels of progesterone and A_4 produced by fresh follicles also increased by Week 3 of culture, but remained similar from Weeks 3 to 6. On the other hand, E_2 and progesterone levels produced by follicles of the VEG group did not rise until Week 6 in culture, whereas the A_4 level increased during Week 2. Even though

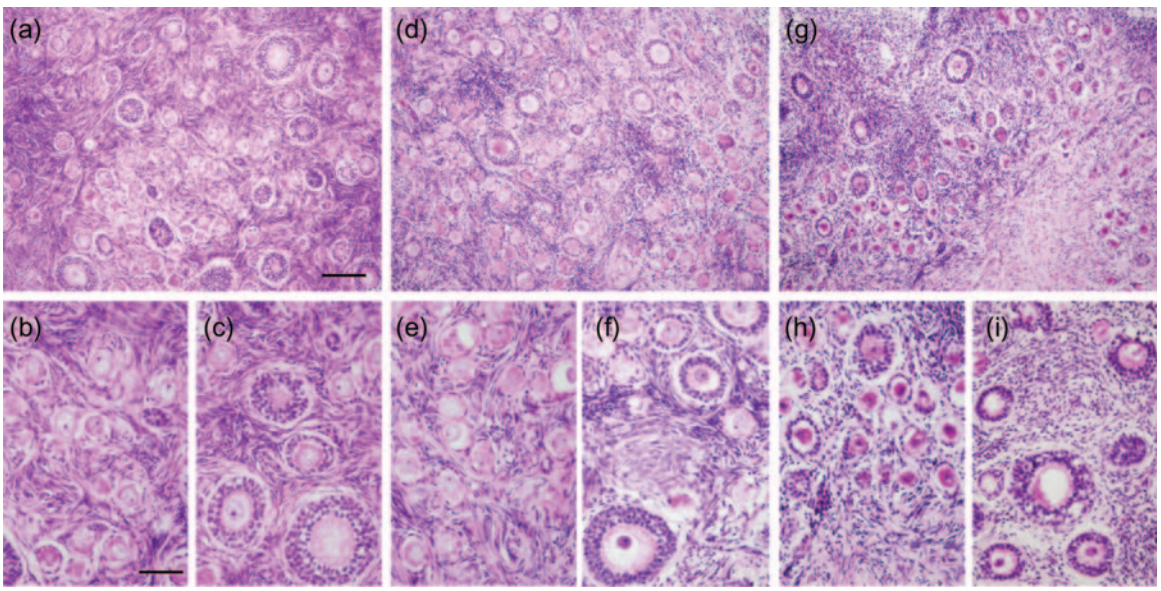

Figure 3 Histology of macaque ovarian tissue. Representative photomicrographs of fixed ovarian tissue from fresh (**a–c**) and vitrified (**d–f** for VEG, **g–l** for VED) tissues. Dense stroma was observed in fresh and vitrified groups (a, d and g). Fresh ovarian tissue showed intact primordial (b), primary (c) and secondary (c) follicles with healthy oocytes and densely compact granulosa cell layers. Following vitrification, morphology of granulosa cells of different classes (e and f) of follicles were mostly preserved in the VEG group; however, some oocytes of primordial, primary and secondary follicles (h and i) seemed shrunken and damaged in the VED group. Scale bar = 100 um (a, d and g), 50 um (b, c, e, f, h and i).

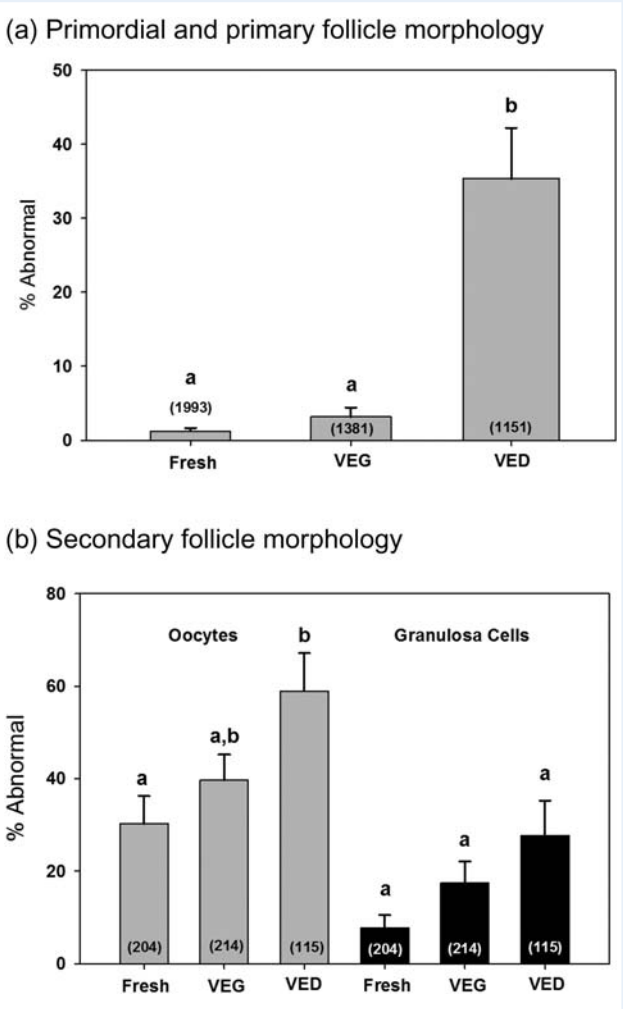

Figure 4 Macaque follicle morphology after vitrification. Percentages (mean ± SEM, $n = 4$) of abnormal primordial and primary follicles (**a**) as well as abnormal oocyte and granulosa cells found in secondary follicles (**b**) of fresh tissue and tissue vitrified with VEG and VED. Numbers inside the bar represent the total number of follicles counted in each group. Different letters on the top of the bar represent significant differences between groups; this means that groups with the same letter are not significantly different from each other; for example, two groups sharing an 'a' denote no significant change between these two groups, whereas 'a' and 'b' denote a significant change between the two groups. The percentage of abnormal primordial and primary follicles as well as oocytes in the secondary follicle was higher in the VED group in comparison with the fresh. No difference in the morphology of granulosa cells in secondary follicles was observed among different groups.

the levels of steroid hormones showed different profiles within the groups between fresh and vitrified follicles, there was no statistically significant change between the groups at any time point during culture, perhaps in part due to the high variability within each group.

Discussion

The combination of glycerol, EG and polymers with reduced cooling and warming rates was able to preserve tissue and follicle morphology as well as function of a small population of secondary follicles in the macaque ovarian cortex following vitrification in a closed system. Vitrification prevents intracellular and extracellular ice formation and may therefore benefit the preservation of ovarian tissue where cell density is high and extracellular connections within the follicle are important (Fahy *et al.*, 2004; Pegg, 2010). Successful vitrification is dependent on various factors including tissue geometry, CPA properties and concentration, as well as cooling and warming rates. The current study benefits from applying principles in both cryobiology and reproductive biology in order to produce an improved condition for ovarian tissue vitrification in a closed system.

For VEG, 54% total permeating CPAs (27% EG and 27% glycerol) was found to be the minimum requirement for apparent vitrification and lack of devitrification for 1 ml of VS in the geometry studied. A lower concentration (51%) of total permeating CPAs was required for VED in comparison with VEG. This is expected, as glycerol is a weaker glass-forming agent than DMSO (Baudot *et al.*, 2000). Our results also showed that the CPA concentration required for a solution to avoid devitrification is higher than that required for a solution to vitrify. The reason is that during cooling, nucleation (the initial process of crystal formation from a solution) tends to take place at temperatures lower than that of the ice growth; therefore, ice cannot grow from the developed nucleation sites. However, during warming, the nuclei are now present in the temperature range for maximum ice crystal growth rates, and ice formation that was successfully avoided during cooling is now favored. The extra CPA is needed to suppress nucleation during cooling and crystal growth during warming. This may be important for future development of VS for large-volume vitrification.

Despite differences in CPA type and concentration, the calculated cooling rates for 1 ml of VEG and VED in LN_2 vapor are similar (~35°C/min). This is relatively slow when compared with the rates used in other vitrification systems [open system: ~20 000°C/min (i.e. CryoTop and Cryoloop) to 100 000°C/min (Kleinhans *et al.*, 2010) and closed system: 1300 (0.25 ml straws) to 12 000°C/min (CryoTip; AbdelHafez *et al.*, 2011)]. The diameter of carriers for closed system vitrification is typically 2 mm or less, too small for ovarian cortex pieces that will be used for transplantation. In the current study, a 2 ml high security straw with an inner diameter of 6 mm was used. Vitrification was observed at −127 and −130°C for VEG and VED, respectively, and no ice crystal formation was observed in both VSs as shown on the DSC cooling scans. When a faster cooling rate was examined by directly plunging the sample into LN_2, extensive fracturing of the sample occurred due to excessive mechanical stress (Fahy *et al.*, 1984; Wowk, 2010).

Similar to the cooling rate examined, two practical (easy to perform) warming rates were tested: a one-step 'fast warming' and a two-step 'slow-then-fast' warming. Extensive fracturing caused by fast warming was resolved by the two-step warming system. The purpose of the slow warming phase is to allow the temperature of the sample to warm above T_g (approximately −115°C during warming) slowly enough so it does not fracture. Measured T_g in this study differed during cooling and warming due to the differences in cooling and warming rates and the thermal lag in the DSC machine. Once the sample becomes a supercool liquid, it is warmed at a faster rate so that the sample does not have sufficient time to devitrify, which has been reported to occur at approximately −50 to −30°C

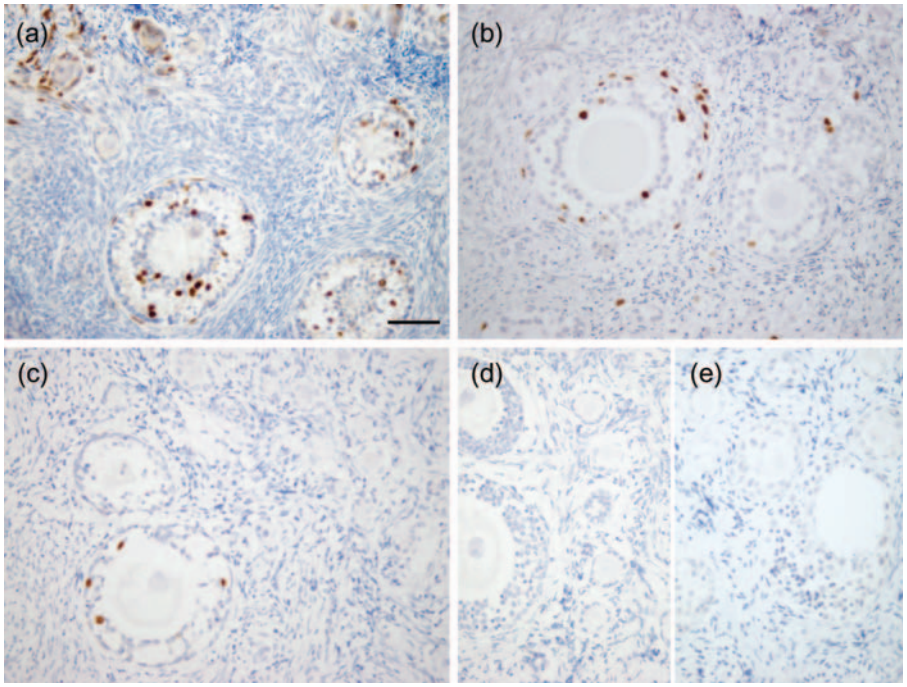

Figure 5 Evaluation of ovarian tissue viability. BrdU uptake was observed in granulosa cells of growing follicles from macaques in fresh (**a**) and tissues vitrified with VEG (**b**) and VED (**c**). Negative controls included primary antibody omission during the staining protocol (**d**) as well as tissue cultured in the absence of BrdU (**e**). Scale bar = 200 μm.

(Mullen *et al.*, 2008). Although high warming rates have been associated with higher survival in oocytes (Seki and Mazur, 2012), in a large-volume tissue system, an ultrarapid warming rate is not achievable and may even be harmful due to fracture-induced physical trauma to the biological specimen. As shown on the DSC thermogram, as well as visually during warming of the straws, devitrification was not observed during the two-step warming for both VSs.

Morphologically, dense stroma was observed in fresh as well as both VEG and VED groups. This is similar to our previous finding, suggesting that vitrification preserved ovarian stroma, while abnormal space was found throughout the stroma following the slow freeze (Ting *et al.*, 2011). The lack of stromal damage following vitrification may be due to the prevention of extracellular ice crystal formation, a situation which is likely to occur during slow freezing (Pegg, 2010). Other studies have also suggested that ovarian stromal integrity is maintained following vitrification (Keros *et al.*, 2009; Silber *et al.*, 2010; Xiao *et al.*, 2010) and damaged following slow freezing (Gook *et al.*, 1999, 2000). While the morphology of pre-antral follicles was preserved following vitrification with VEG, follicular abnormality was observed more frequently in the VED vitrified tissue when compared with fresh controls. This may be due to toxicity caused by DMSO in comparison with glycerol. DMSO has been found to cause irreversible disruption of the microtubular system in mouse oocytes (Johnson and Pickering, 1987). While others have shown promising results using DMSO and EG for ovarian tissue vitrification (Kagawa *et al.*, 2009), the CPA concentration in the current studies (7.5 M) was higher than that (4.5 M) used in an open system and may be the reason for follicular toxicity. It is unlikely that our results are due to lower penetration of DMSO, since glycerol has been shown to be less permeable than EG and DMSO in primordial follicles as well as germinal vesicle and metaphase II oocytes (Songsasen *et al.*, 2002; Amorim *et al.*, 2006). Uptake of BrdU, a marker for chromosomal replication during the S-phase of mitosis (Gratzner, 1982), was examined in cultured tissues as an indicator for short-term granulosa cell viability. Despite some levels of follicular abnormality, BrdU uptake was observed in the granulosa cells of growing follicles in fresh and both vitrified groups, suggesting intact short-term functions of some granulosa cells even in vitrified tissues. Indeed, based on our histological observation, follicular damage following vitrification is mostly associated with the oocyte and not granulosa cells.

Table I Survival (at 6 weeks) and antrum formation during 3D culture of encapsulated follicles isolated from fresh and vitrified tissues taken from the non-human primate

	Fresh	VEG
Average (total number of follicles)	18 ± 3 (72)	30 ± 6 (120)
% Survival rate	70 ± 12 (46)	52 ± 2 (63)
% Antrum formation rate	64 ± 8 (29)	37 ± 6 (25)*

Data represent the average number (mean ± SEM, per animal, $n = 4$ animals) of secondary follicles and their survival rates (%) and the ability to form antrum (%) among those that survived. Data in parentheses represent the total number of follicles. Data were analyzed using one way analysis of variance.
*Significant difference ($P \leq 0.05$) in comparison to the fresh group.

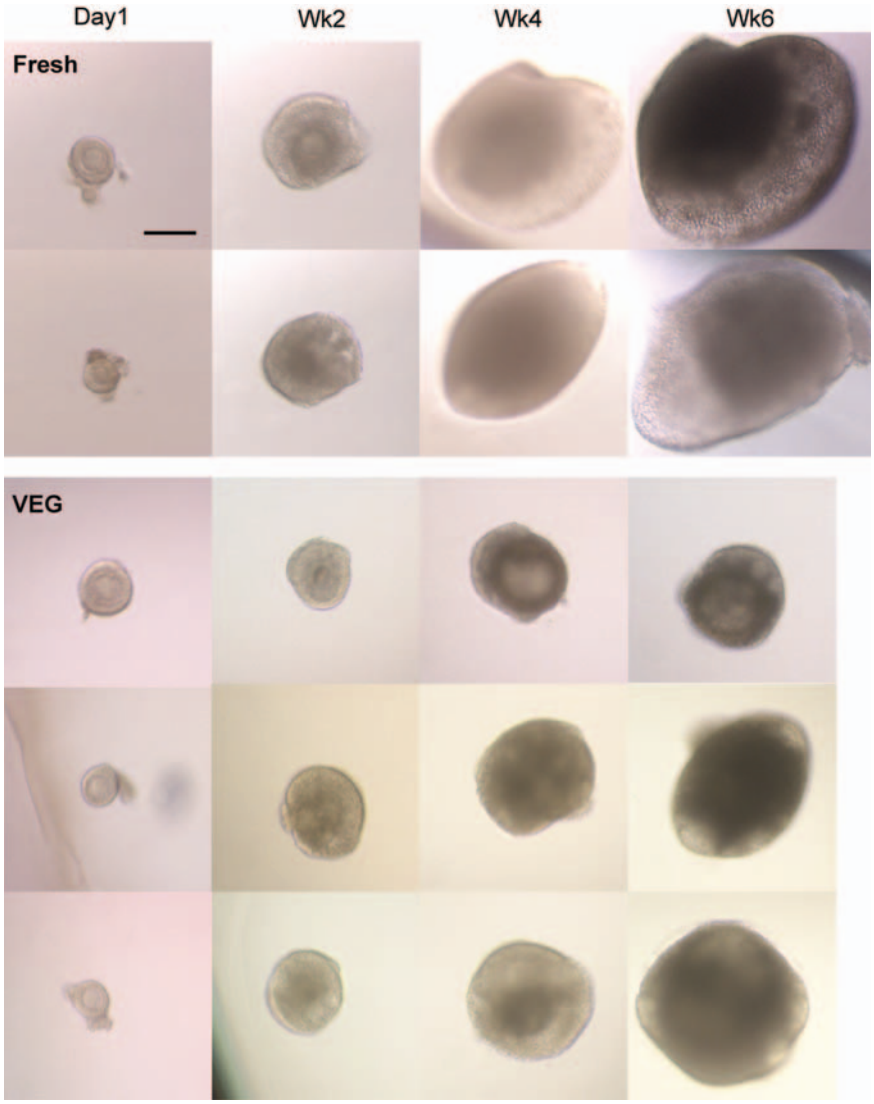

Figure 6 Culture of secondary follicles after vitrification. Representative pictures of isolated secondary macaque follicles from fresh and tissue vitrified with VEG during 6 weeks of culture. Follicles isolated from fresh tissues grew in size in 6 weeks of culture and formed an antrum by Weeks (WK) 3 and 4. Follicles isolated from VEG tissues showed delayed growth but some were able to form an antrum. Scale bar = 250 um.

Growth and hormone production of intact secondary follicles showed that vitrification with VEG maintained long-term follicular function *in vitro*. In addition to serving as a functional end-point, successful *in vitro* maturation (IVM) of follicles from vitrified tissue can offer patients whose ovarian tissue contains malignant cells an option for fertility preservation because tissue grafting and *in vivo* growth may cause cancer reoccurrence. In primates, mature oocytes that are capable of fertilization and early embryonic development have only been demonstrated from secondary follicles of fresh ovarian tissue using a 3D culture system (Xu *et al.*, 2010, 2011). During normal *in vivo* and *in vitro* development, the size of a secondary follicle increases due to the rapid proliferation of granulosa cells and increased oocyte diameter. This growth is associated with antrum formation and elevated levels E_2 production by granulosa cells, as well as progesterone and A_4 productions by theca cells. In the current study, vitrified follicles showed an increase in diameter in culture and produced similar levels of steroid hormones in comparison with those of the control follicles from fresh tissue, indicating viable granulosa cells. While no significant difference in levels of hormone production was found between fresh and VEG groups, production of E_2, progesterone and A_4 in VEG follicles seemed to be delayed when compared with the fresh follicles. This delay seems to correlate with follicular growth. Despite a similar follicular survival rate in the fresh and vitrified groups, the antrum formation rate was lower in follicles from vitrified tissue in comparison to the control. Although somatic (granulosa and theca) cells are responsible for producing steroid hormones and forming an antrum, signals from the oocyte are also critical for somatic cell action. The exact mechanism of how vitrification causes follicular damage is still unclear.

One inconsistency among studies for ovarian tissue vitrification is the size of the ovarian cortex. Although studies agree that tissue thickness is critical and thinner tissues are favored due to faster CPA

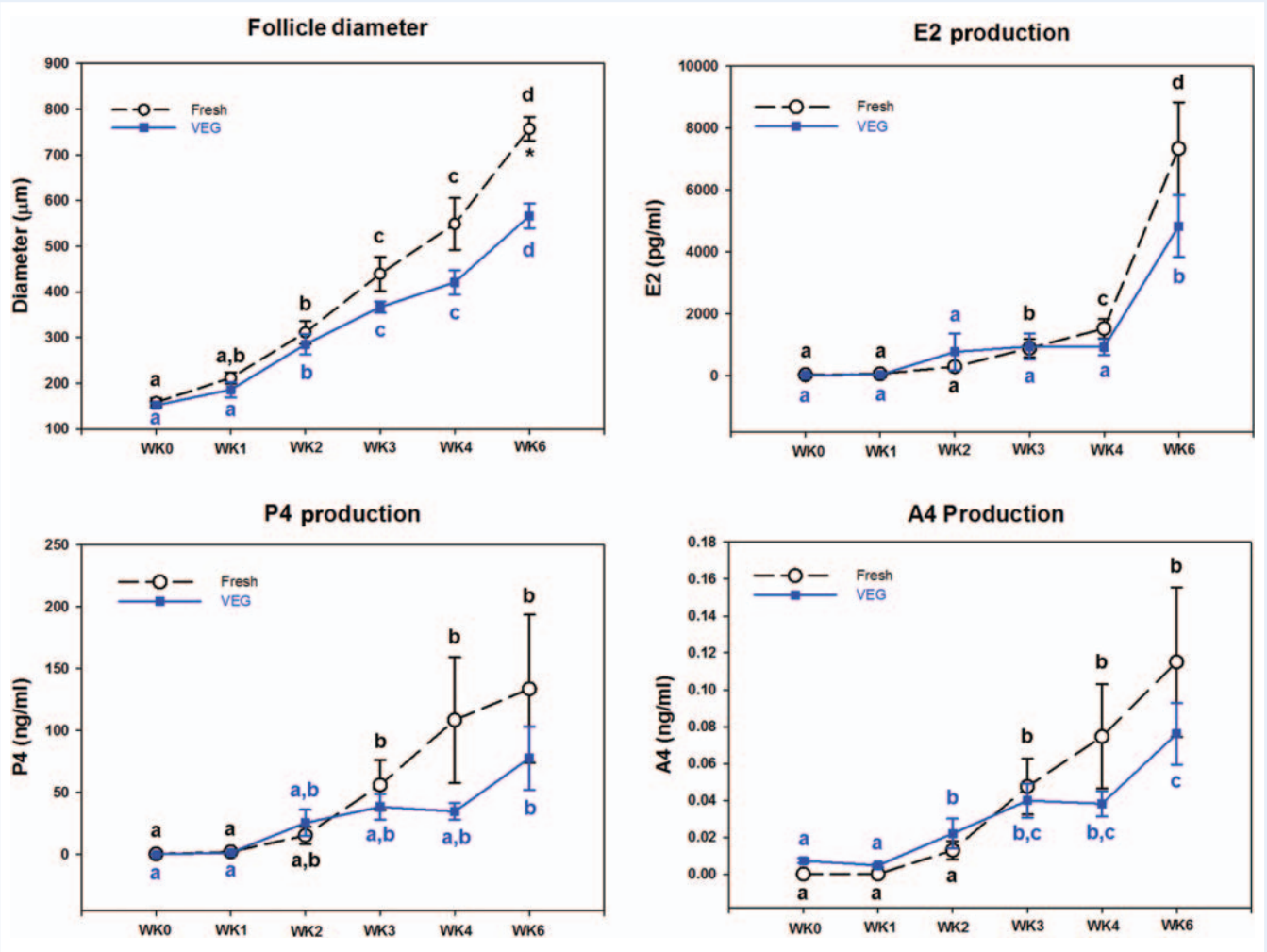

Figure 7 Weekly follicle diameter and steroid hormone production (estradiol, E_2; progesterone, P_4; and androstenedione, A_4) during 6 weeks in culture. Data are presented as the mean ± SEM of follicles isolated from macaques ($n = 4$ animals, 12–24/group/animal) that survived (Table I). Different letters above data points represent significant changes from one week to another within the same group over 6 weeks in culture. This means that groups with the same letter are not significantly different from each other; for example, two groups sharing an 'a' denote no significant change between these two groups, whereas 'a' and 'b' denote a significant change between the two groups. Asterisks represent significant changes among different groups within a given week of culture.

penetration (lower toxicity) and cooling/warming rates, almost all studies use scalpels or scissors to create an approximately 1 mm thickness without accuracy and consistency. In the current study, we utilized a tissue slicer to produce 0.5 mm thick tissue pieces. Using the slicer, multiple layers of the ovary can be preserved for different purposes. The outermost layer of the ovary contains primordial and most of the primary follicles and can be used for future transplantation, whereas the second layer of the ovarian cortex typically contains some primary and most secondary follicles and can be used for follicle isolation and IVM.

As described in our previous publication (Ting *et al.*, 2012), a challenge remains when using histology to evaluate survival and viability of cryopreserved ovarian tissue (Gook and Edgar, 2011). In primates, follicular density varies within the ovarian cortex (Schmidt *et al.*, 2003). Once cut into fragments, each cortical tissue contains different numbers and classes of ovarian follicles prior to cryopreservation and unless these can be quantified prior to treatment, it will be inaccurate to compare the absolute number of follicles among different groups. In addition, since follicles that lyse during the cryopreservation procedure would not be detected during analysis, interpretation of the proportional data should also be done with caution.

Possibilities for specimen contamination during processing and storage from direct contact of tissue with LN_2 have been a concern for ovarian tissue cryopreservation. Human ovarian fragments vitrified in a cryotube and stored in LN_2 vapor has been described as a closed system (Sheikhi *et al.*, 2011). However, whether or not a true closed system can be achieved inside a cryotube is still unclear because there is a possibility of LN_2 or airborne contaminants leaking into the vial during LN_2 or LN_2 vapor storage (Grout and Morris, 2009; Mirabet *et al.*, 2012). A recent report by Suzuki *et al.* (2012) investigated ovarian function following heterotopic transplantation of macaque ovarian tissue vitrified in an open or closed system. The authors

showed a return of ovarian function using both systems, but only the open system yielded mature oocytes. Furthermore, the closed system used in the Suzuki study consisted of 0.5 ml sealable straws containing $1 \times 1 \times 1$ mm^3 tissue pieces. Since we have now determined the limiting concentration for 1 ml of VS to vitrify in a sealed straw, theoretically, as long as the tissue is saturated with the VS and can fit into the same configuration (6×60 mm^2), regardless of its size it will vitrify. Further development of closed system vitrification will require optimization for the larger pieces of tissue used for transplantation.

Collectively, we have demonstrated in the current study that the morphology and function of pre-antral follicles can be preserved after vitrification using glycerol, EG and synthetic polymers in macaque ovarian tissue. Under optimized conditions, secondary follicles isolated from vitrified ovarian tissue display survival, growth, antrum formation and steroid production in a 3D culture system. The combination of successful ovarian tissue cryopreservation with IVM of pre-antral follicles may provide a safe alternative for fertility preservation, especially for patients who are prepubertal or for those who have possible cancer cells in the ovary. The current study is the first to characterize a true closed system for primate ovarian tissue vitrification based on the stability of the VS against ice formation. However, results from tissue histology, short-term tissue culture and long-term follicle culture may not reflect fertility potential, which can only be evaluated after tissue transplantation or when mature competent oocytes can be obtained from 3D follicle culture. The non-human primate serves as an important model for the continuation of optimizing ovarian tissue cryopreservation protocols that can be translated directly into clinical use.

Acknowledgements

We thank Mr Ernest Basarah (21st Century Medicine) for performing the thermoscans for the vitrification solution and his expert advice. We would like to acknowledge Dr Francis Pau and the ONPRC Endocrine Technology and Support Core for performing hormone assay and Ms Barbra Mason for tissue processing and sectioning. In addition, we are grateful to the Comparative Medicine for performing surgeries Animal Resources excellent animal care.

Authors' roles

A.Y.T. and M.B.Z were involved in the experimental conception and design, execution, data acquisition, interpretation and analysis as well as manuscript preparation and revision. R.R.Y., J.R.C. and M.S.L. were involved in the experimental conception and design, execution, data acquisition, interpretation and analysis as well as manuscript revision. S.F.M and G.M.F were involved in the experimental conception and design, analysis, critical discussion and manuscript revision. All authors have approved the final version and submission of this manuscript.

Funding

This work was supported by the National Institute of Child Health and Human Development (NICHD)/National Institutes of Health (NIH) Oncofertility Consortium UL1 RR024926 (1RL1-HD058293, HD058295 and PL1 EB008542), the Eunice Kennedy Shriver NICHD/NIH through cooperative agreement (U54 HD018185) and ONPRC 8P51OD011092-53.

Conflict of interest

A.Y.T., R.R.Y., J.R.C., M.S.L., S.F.M and M.B.Z have none to declare. G.M.F. works for the company that makes the polymers used in the current study.

References

Abdelhafez FF, Desai N, Abou-Setta AM, Falcone T, Goldfarb J. Slow freezing, vitrification and ultra-rapid freezing of human embryos: a systematic review and meta-analysis. *Reprod Biomed Online* 2010; **2**:209–222.

AbdelHafez F, Xu J, Goldberg J, Desai N. Vitrification in open and closed carriers at different cell stages: assessment of embryo survival, development, DNA integrity and stability during vapor phase storage for transport. *BMC Biotechnol* 2011:**29**:1–10.

Ali J, Shelton JN. Design of vitrification solutions for the cryopreservation of embryos. *J Reprod Fertil* 1993;**2**:471–477.

Amorim CA, Rondina D, Lucci CM, Goncalves PB, Figueiredo JR, Giorgetti A. Permeability of ovine primordial follicles to different cryoprotectants. *Fertil Steril* 2006:**85**(Suppl. 1):1077–1081.

Amorim CA, Curaba M, Van Langendonckt A, Dolmans MM, Donnez J. Vitrification as an alternative means of cryopreserving ovarian tissue. *Reprod Biomed Online* 2011;**2**:160–186.

Amorim CA, Dolmans MM, David A, Jaeger J, Vanacker J, Camboni A, Donnez J, Van Langendonckt A. Vitrification and xenografting of human ovarian tissue. *Fertil Steril* 2012;**5**:1291–1298, e1291–e1292.

Baudot A, Alger L, Boutron P. Glass-forming tendency in the system water-dimethyl sulfoxide. *Cryobiology* 2000;**2**:151–158.

Bielanski A, Vajta G. Risk of contamination of germplasm during cryopreservation and cryobanking in IVF units. *Hum Reprod* 2009; **10**:2457–2467.

Cobo A, Diaz C. Clinical application of oocyte vitrification: a systematic review and meta-analysis of randomized controlled trials. *Fertil Steril* 2011;**2**:277–285.

de Graaf IA, Draaisma AL, Schoeman O, Fahy GM, Groothuis GM, Koster HJ. Cryopreservation of rat precision-cut liver and kidney slices by rapid freezing and vitrification. *Cryobiology* 2007;**1**:1–12.

Demeestere I, Simon P, Moffa F, Delbaere A, Englert Y. Birth of a second healthy girl more than 3 years after cryopreserved ovarian graft. *Hum Reprod* 2010;**6**:1590–1591.

Donnez J, Jadoul P, Pirard C, Hutchings G, Demylle D, Squifflet J, Smitz J, Dolmans MM. Live birth after transplantation of frozen-thawed ovarian tissue after bilateral oophorectomy for benign disease. *Fertil Steril* 2012; **3**:720–725.

Fahy GM, MacFarlane DR, Angell CA, Meryman HT. Vitrification as an approach to cryopreservation. *Cryobiology* 1984;**4**:407–426.

Fahy GM, Wowk B, Wu J, Phan J, Rasch C, Chang A, Zendejas E. Cryopreservation of organs by vitrification: perspectives and recent advances. *Cryobiology* 2004;**2**:157–178.

Gook DA, Edgar DH. Ovarian tissue cryopreservation. In Donnez J, Kim SS (eds) *Principles and Practice of Fertility Preservation*. New York, USA: Cambridge University Press, 2011, 342–356.

Gook DA, Edgar DH, Stern C. Effect of cooling rate and dehydration regimen on the histological appearance of human ovarian cortex following cryopreservation in 1, 2-propanediol. *Hum Reprod* 1999; **8**:2061–2068.

Gook DA, Edgar DH, Stern C. The effects of cryopreservation regimens on the morphology of human ovarian tissue. *Mol Cell Endocrinol* 2000; **1–2**:99–103.

Gougeon A. Regulation of ovarian follicular development in primates: facts and hypotheses. *Endocr Rev* 1996;**2**:121–155.

Gratzner HG. Monoclonal antibody to 5-bromo- and 5-iododeoxyuridine: A new reagent for detection of DNA replication. *Science* 1982; **4571**:474–475.

Grout BW, Morris GJ. Contaminated liquid nitrogen vapour as a risk factor in pathogen transfer. *Theriogenology* 2009;**7**:1079–1082.

Hashimoto S, Suzuki N, Yamanaka M, Hosoi Y, Ishizuka B, Morimoto Y. Effects of vitrification solutions and equilibration times on the morphology of cynomolgus ovarian tissues. *Reprod Biomed Online* 2010;**4**:501–509.

Howlader N, Noone A, Krapcho M, Neyman N, Aminou R, Altekruse S, Kosary C, Ruhl J, Tatalovich Z, Cho H *et al.* 2012. *SEER Cancer Statistics Review, 1975–2009 (Vintage 2009 Populations)*. National Cancer Institute.

Isachenko V, Isachenko E, Rahimi G, Krivokharchenko A, Alabart JL, Nawroth F. Cryopreservation of human ovarian tissue by direct plunging into liquid nitrogen: negative effect of disaccharides in vitrification solution. *Cryo Letters* 2002;**5**:333–344.

Jeruss JS, Woodruff TK. Preservation of fertility in patients with cancer. *N Engl J Med* 2009;**9**:902–911.

Johnson MH, Pickering SJ. The effect of dimethylsulphoxide on the microtubular system of the mouse oocyte. *Development* 1987; **2**:313–324.

Kagawa N, Silber S, Kuwayama M. Successful vitrification of bovine and human ovarian tissue. *Reprod Biomed Online* 2009;**4**:568–577.

Keros V, Xella S, Hultenby K, Pettersson K, Sheikhi M, Volpe A, Hreinsson J, Hovatta O. Vitrification versus controlled-rate freezing in cryopreservation of human ovarian tissue. *Hum Reprod* 2009; **7**:1670–1683.

Kleinhans FW, Seki S, Mazur P. Simple, inexpensive attainment and measurement of very high cooling and warming rates. *Cryobiology* 2010;**2**:231–233.

Martinez-Burgos M, Herrero L, Megias D, Salvanes R, Montoya MC, Cobo AC, Garcia-Velasco JA. Vitrification versus slow freezing of oocytes: effects on morphologic appearance, meiotic spindle configuration, and DNA damage. *Fertil Steril* 2011;**1**:374–377.

Mazur P. Principles of Cryobiology. In Fuller BJ, Lane N, Benson EE (eds) *Life in the Frozen State*, Chapter 1. Boca Raton, Florida: CRC Press, 2004, 3–65.

Mirabet V, Alvarez M, Solves P, Ocete D, Gimeno C. Use of liquid nitrogen during storage in a cell and tissue bank: contamination risk and effect on the detectability of potential viral contaminants. *Cryobiology* 2012;**2**:121–123.

Mullen SF, Li M, Li Y, Chen ZJ, Critser JK. Human oocyte vitrification: the permeability of metaphase II oocytes to water and ethylene glycol and the appliance toward vitrification. *Fertil Steril* 2008;**6**:1812–1825.

Muller A, Keller K, Wacker J, Dittrich R, Keck G, Montag M, Van der Ven H, Wachter D, Beckmann MW, Distler W. Retransplantation of cryopreserved ovarian tissue: the first live birth in Germany. *Dtsch Arztebl Int* 2012;**1–2**:8–13.

Onions VJ, Mitchell MR, Campbell BK, Webb R. Ovarian tissue viability following whole ovine ovary cryopreservation: assessing the effects of sphingosine-1-phosphate inclusion. *Hum Reprod* 2008;**3**:606–618.

Pegg DE. The relevance of ice crystal formation for the cryopreservation of tissues and organs. *Cryobiology* 2010;**60**(Suppl 3):S36–44.

Poirot C, Abirached F, Prades M, Coussieu C, Bernaudin F, Piver P. Induction of puberty by autograft of cryopreserved ovarian tissue. *Lancet* 2012;**9815**:588.

Rosendahl M, Schmidt KT, Ernst E, Rasmussen PE, Loft A, Byskov AG, Andersen AN, Andersen CY. Cryopreservation of ovarian tissue for a decade in Denmark: a view of the technique. *Reprod Biomed Online* 2011;**2**:162–171.

Schmidt KL, Byskov AG, Nyboe Andersen A, Muller J, Yding Andersen C. Density and distribution of primordial follicles in single pieces of cortex from 21 patients and in individual pieces of cortex from three entire human ovaries. *Hum Reprod* 2003;**6**:1158–1164.

Schmidt KT, Larsen EC, Andersen CY, Andersen AN. Risk of ovarian failure and fertility preserving methods in girls and adolescents with a malignant disease. *BJOG* 2010;**2**:163–174.

Seki S, Mazur P. Ultra-rapid warming yields high survival of mouse oocytes cooled to -196 degrees c in dilutions of a standard vitrification solution. *PLoS One* 2012;**4**:e36058.

Sheikhi M, Hultenby K, Niklasson B, Lundqvist M, Hovatta O. Clinical grade vitrification of human ovarian tissue: an ultrastructural analysis of follicles and stroma in vitrified tissue. *Hum Reprod* 2011; **3**:594–603.

Silber SJ. Ovary cryopreservation and transplantation for fertility preservation. *Mol Hum Reprod* 2012;**2**:59–67.

Silber S, Kagawa N, Kuwayama M, Gosden R. Duration of fertility after fresh and frozen ovary transplantation. *Fertil Steril* 2010; **6**:2191–2196.

Songsasen N, Ratterree MS, VandeVoort CA, Pegg DE, Leibo SP. Permeability characteristics and osmotic sensitivity of rhesus monkey (*Macaca mulatta*) oocytes. *Hum Reprod* 2002;**7**:1875–1884.

Suzuki N, Hashimoto S, Igarashi S, Takae S, Yamanaka M, Yamochi T, Takenoshita M, Hosoi Y, Morimoto Y, Ishizuka B. Assessment of long-term function of heterotopic transplants of vitrified ovarian tissue in cynomolgus monkeys. *Hum Reprod* 2012;**8**:2420–2429.

Ting AY, Yeoman RR, Lawson MS, Zelinski MB. In vitro development of secondary follicles from cryopreserved rhesus macaque ovarian tissue after slow-rate freeze or vitrification. *Hum Reprod* 2011; **9**:2461–2472.

Ting AY, Yeoman RR, Lawson MS, Zelinski MB. Synthetic polymers improve vitrification outcomes of macaque ovarian tissue as assessed by histological integrity and the in vitro development of secondary follicles. *Cryobiology* 2012;**1**:1–11.

Wolf DP, Thomson JA, Zelinski-Wooten MB, Stouffer RL. In vitro fertilization-embryo transfer in nonhuman primates: the technique and its applications. *Mol Reprod Dev* 1990;**3**:261–280.

Wowk B. Thermodynamic aspects of vitrification. *Cryobiology* 2010; **1**:11–22.

Wowk B, Leitl E, Rasch CM, Mesbah-Karimi N, Harris SB, Fahy GM. Vitrification enhancement by synthetic ice blocking agents. *Cryobiology* 2000;**3**:228–236.

Xiao Z, Wang Y, Li L, Luo S, Li SW. Needle immersed vitrification can lower the concentration of cryoprotectant in human ovarian tissue cryopreservation. *Fertil Steril* 2010;**6**:2323–2328.

Xu J, Bernuci MP, Lawson MS, Yeoman RR, Fisher TE, Zelinski MB, Stouffer RL. Survival, growth, and maturation of secondary follicles from prepubertal, young, and older adult rhesus monkeys during encapsulated three-dimensional culture: effects of gonadotropins and insulin. *Reproduction* 2010;**5**:685–697.

Xu J, Lawson MS, Yeoman RR, Pau KY, Barrett SL, Zelinski MB, Stouffer RL. Secondary follicle growth and oocyte maturation during encapsulated three-dimensional culture in rhesus monkeys: effects of gonadotrophins, oxygen and fetuin. *Hum Reprod* 2011; **5**:1061–1072.

Yavin S, Arav A. Measurement of essential physical properties of vitrification solutions. *Theriogenology* 2007;**1**:81–89.